Histochem Cell Biol (2016) 146:695–707
DOI 10.1007/s00418-016-1502-z

REVIEW

Using electron microscopes to look into the lung

Matthias Ochs[1,2,3] · Lars Knudsen[1,2,3] · Jan Hegermann[1,3] · Christoph Wrede[1,3] · Roman Grothausmann[1,3] · Christian Mühlfeld[1,2,3]

Accepted: 20 September 2016 / Published online: 29 September 2016

Abstract In the nineteenth century, there was a dispute about the existence of a lung alveolar epithelium which remained unsolved until the invention of electron microscopy (EM) and its application to the lung. From the early 1960s, Ewald Weibel became the master of lung EM. He showed that the alveolar epithelium is covered with a lining layer containing surfactant. Weibel also explained the phenomenon of "non-nucleated plates" observed already in 1881 by Albert Kölliker. Weibel's most significant contribution was to the development of stereological methods. Therefore, quantitative characterization of lung structure revealing structure–function relationships became possible. Today, the spectrum of EM methods to study the fine structure of the lung has been extended significantly. Cryo-preparation techniques are available which are necessary for immunogold labeling of molecules. Energy-filtering techniques can be used for the detection of elements. There have also been major improvements in stereology, thus providing a very versatile toolbox for quantitative lung phenotype analyses. A new dimension was added by 3D EM techniques. Depending on the desired sample size and resolution, the spectrum ranges from array tomography via serial block face scanning EM and focused ion beam scanning EM to electron tomography. These 3D datasets provide new insights into lung ultrastructure. Biomedical EM is an ever-developing field. Its high resolution remains unparalleled. Moreover, EM has the unique advantage of providing an "open view" into cells and tissues within their full architectural context. Therefore, EM will remain an indispensable tool for a better understanding of the lung's functional design.

Keywords Electron microscopy · Volume EM · Stereology · Type II alveolar epithelial cell · Surfactant · Fibrosis · Collapse induration

A look back ("retrospectroscope")

Scientific progress critically depends on the development of new or improved analytical instruments. Visualization is an essential way to gain scientific knowledge. Microscopes enable to visualize and resolve objects that are otherwise not accessible to the human eye. They are a paradigmatic example for scientific instruments because they symbolize meticulous investigation and attention to detail which lead to new findings and, in the truest sense of the word, to new insights. Every scientific field has a particular history, and for a thorough understanding of the current state, it is necessary to look back into the past. This "instrument" has been termed "retrospectroscope" (Comroe 1977), and we will use it to look back into the history of lung microscopy (see also Weibel 1996, for an elegant review).

Dedicated to Detlev Drenckhahn on the occasion of his retirement as Editor-in-Chief of Histochemistry and Cell Biology.

Electronic supplementary material The online version of this article (doi:10.1007/s00418-016-1502-z) contains supplementary material, which is available to authorized users.

✉ Matthias Ochs
ochs.matthias@mh-hannover.de

[1] Institute of Functional and Applied Anatomy, Hannover Medical School, Carl-Neuberg-Str. 1, 30625 Hannover, Germany

[2] Biomedical Research in Endstage and Obstructive Lung Disease Hannover (BREATH), Member of the German Center for Lung Research (DZL), Hannover, Germany

[3] REBIRTH Cluster of Excellence, Hannover, Germany

Is there an alveolar epithelium?

The major function of the mammalian lung is gas exchange. It is optimized to perform this function by providing a large surface area and a thin barrier for diffusion of oxygen and carbon dioxide between air (alveolar airspaces) and blood (alveolar capillaries) (Ochs and Weibel 2015; Hsia et al. 2016). But how is this air–blood barrier built in detail? From the early days of histology in the nineteenth century, there was a dispute whether or not an epithelium covering lung alveolar capillaries exists. This dispute remained unsolved until the middle of the twentieth century. A major contribution came from Albert Kölliker (1817–1905). In 1881, Kölliker, at that time professor of anatomy and physiology at the University of Würzburg, published a paper entitled "Zur Kenntniss des Baues der Lunge des Menschen" (Kölliker 1881). Based on careful light microscopic examinations of samples obtained from only one human lung and using silver nitrate for staining intercellular junctions, Kölliker found the epithelium "wenn auch vollständig und zusammenhängend, doch nicht gleichartig" (although complete and continuous, not uniform). He went even further and described two elements: small nucleated spherical to polygonal cells and large cell plates covering the capillaries which seemed to have no nucleus ("kernlose Platten" or "non-nucleated plates"). Köllikers findings and interpretations were later supported by some but also criticized by others. While some histologists denied the existence of an alveolar epithelium, stating that the capillaries are "naked" to facilitate gas exchange (e.g., Albert Policard from the University of Lyon), others claimed that there is an epithelium, either continuous or initially continuous but later fragmented due to lung expansion during development (e.g., Charles C. Macklin from the University of Western Ontario and William S. Miller from the University of Wisconsin). The state of knowledge around the middle of the twentieth century was summarized by Miller in his seminal monograph "The lung" (Miller 1937). Miller refers to the 1936 meeting of the American Association of Anatomists, where the presence or absence of an alveolar epithelium was the subject of a round table conference. He quotes the report of the chairman of this conference, Charles C. Macklin: "no conclusions were drawn by the Conference." The reason why this case could not be closed was simple: the resolution of light microscopy was too limited to clarify this issue.

The final answer came with the invention of electron microscopy (EM) and its application to the lung. In the early 1950s, Frank Low (1911–1998), the "gentle giant of electron microscopy" (Carlson 1999), convincingly demonstrated the presence of a continuous alveolar epithelium (Low 1952, 1953). Today we know that this epithelium is, as anticipated already by Kölliker in 1881, a mosaic of two different cell types, now designated as type I and type II alveolar epithelial cells. Type I cells possess thin cytoplasmic sheets of only 0.1- to 0.2-µm thickness, thus beyond the resolution limit of conventional light microscopy. Type II cells are secretory cuboidal cells that also serve as progenitor cells of the alveolar epithelium (see Weibel 1996, 2015; West 2016, for review). By this mosaic, the two main tasks for epithelial cells are divided: the lining function (type I cells) and the secretory function (type II cells).

Ewald Weibel: measuring lung structure

From the early 1960s, Ewald Weibel (born in 1929) became the master of lung EM. After graduating from Medical School and training in Anatomy and Histology at the University of Zürich, he worked in the laboratories of André Cournand, Dickinson Richards and George Palade in New York from 1959 to 1963. Cournand and Richards had received the Nobel prize in 1956; Palade later received it in 1974. Weibel returned to Zürich in 1963 and became chair of the Institute of Anatomy at the University of Bern in 1966. Using "fixation from behind" (i.e., vascular perfusion), Weibel showed that even the alveolar epithelium is not naked but covered with a duplex lining layer consisting of an extremely thin surface film and an aqueous hypophase containing surfactant (Weibel and Gil 1968; Gil and Weibel 1969/1970). Surfactant, a surface active agent (hence the acronym) synthesized and secreted by type II alveolar epithelial cells and required to prevent alveoli from collapsing, was characterized earlier biophysically by John Clements (Clements 1957, 1997). A specific intraalveolar surfactant subtype with a typical lattice-like structure was first described by Weibel and termed "tubular myelin" (Weibel et al. 1966). Weibel also explained the phenomenon of "non-nucleated plates" observed by Kölliker in 1881 by showing that type I alveolar epithelial cells are capable of sending cell extensions through the alveolar septal wall onto the opposite side of the septum (where the epithelium lines a neighboring alveolus and where these cell extensions seemingly have no nucleus) (Weibel 1971). Moreover, together with George Palade, he described a new organelle in pulmonary arterial endothelial cells which was later termed "Weibel-Palade body" (Weibel and Palade 1964). A most significant contribution to microscopy by Ewald Weibel was to the development of stereological methods (Weibel and Gomez 1962; Weibel 1963, 1979a, 1980, 2013). Derived from the sound mathematical principles of stochastic geometry, stereology provides methods for quantitative assessment of objects in microscopy. In cases when, due to the size of the object and the microscopic technique, only parts of the object can be analyzed (i.e., a reduction in sample size is necessary) and when only nearly two-dimensional (virtual or physical) sections

through the three-dimensional object can be analyzed (i.e., a reduction in dimension is necessary), stereology is the method of choice. Using rigorous sampling and measurement protocols, accurate (unbiased) and precise quantitative 3D data can be obtained efficiently from microscopic sections (for historic review, see Cruz-Orive 1987; Weibel 1992). Stereology thus adds hard data to nice micrographs and therefore extends qualitative morphologic description to quantitative morphometric measurement at the microscopic level. Applied to the lung, quantitative data characterizing its inner structure (e.g., the surface area of the alveolar epithelium or the thickness of the air–blood barrier) were generated and used to reveal structure–function relationships (e.g., Weibel 1973, 1979b, 1984).

The current status

Extending and refining the tools

Today, the spectrum of EM methods available to study the fine structure of the lung has been extended significantly (Koster and Klumperman 2003; McIntosh 2007; Allen 2008; Kuo 2014). Besides conventional chemical fixation, cryo-preparation techniques are available (Cavalier et al. 2009). They include cryo-fixation, e.g., vitrification without ice crystal formation of samples of up to 200 µm by high-pressure freezing (Moor et al. 1980; Studer et al. 2001, 2008). These samples can then undergo either post-fixation, dehydration or low-temperature embedding by freeze substitution followed by ultrathin sectioning at room temperature or ultrathin cryo-sectioning (Mühlfeld et al. 2007). A "chemical-free" protocol that involves high-pressure freezing, ultrathin cryo-sectioning of frozen hydrated samples and EM analysis under cryo-conditions is termed CEMOVIS (cryo-electron microscopy of vitreous sections) (Al-Amoudi et al. 2004; Studer et al. 2008; Dubochet 2012). The CEMOVIS technique has been applied to study the ultrastructure of surfactant-containing lamellar bodies in type II alveolar epithelial cells under conditions as close as possible to the in vivo state (Vanhecke et al. 2010) Cryo-methods are also important for improved preservation of antigenicity, thus allowing for immunolabeling of molecules using colloidal gold as marker system (Roth et al. 1978, 1981; Roth 1989, 1996; Bendayan 2001; Möbius 2009). Suitable samples are, for example, prepared by freeze substitution or by the Tokuyasu technique (Griffiths 1993; Liou et al. 1996). Applied to the lung, the intracellular and intraalveolar localization of surfactant proteins as well as their posttranslational processing could be analyzed in detail (Voorhout et al. 1993; Ochs et al. 2002; Brasch et al. 2002, 2003, 2004). Because colloidal gold particles are "countable," they are ideally suited as a readout for quantitative analysis of immunolabeling by stereology (Bendayan et al. 1980; Mühlfeld et al. 2007; Mayhew and Lucocq 2008; Mayhew et al. 2009; Mayhew 2015). This is of particular importance for very weak signals in order to check whether "those few gold particles" (Griffiths 1993) represent a preferential labeling or just unspecific background. Using this approach, the preferential localization of surfactant protein A to lamellar bodies in the human lung could be shown although an average of only two immunogold particles per cell was found over lamellar bodies (Ochs et al. 2002). Energy-filtering techniques can be used for the detection of (endogenous or tracer) elements (Bauer 1988; Leapman and Ornberg 1988; Reimer 1991), e.g., for analysis of the composition of lamellar bodies in type II alveolar epithelial cells (Ochs et al. 1994; Fehrenbach et al. 1995; Ochs et al. 2001, 2004a).

There have also been major improvements in stereological theory and practice (Baddeley and Vedel Jensen 2005; Howard and Reed 2005), thus providing a very versatile toolbox for quantitative lung phenotype analyses of gene-manipulated organisms and animal models of human lung disease. Design-based stereological methods are universally applicable and can be combined with any imaging device—from macro- to nanoscale. The application of stereology to the lung has been reviewed in detail (Ochs 2006a, b; Weibel et al. 2007; Ochs and Mühlfeld 2013; Mühlfeld and Ochs 2013; Mühlfeld et al. 2015; Brandenberger et al. 2015). Lung stereology has been standardized by an official research policy statement of the American Thoracic Society and the European Respiratory Society (Hsia et al. 2010). Particular examples include the application of the disector method (Sterio 1984) for estimation of the number of type II alveolar epithelial cells in the lung and, at the EM level, the number of their surfactant-containing lamellar bodies (Ochs et al. 2004b; Jung et al. 2005). The disector method, originally developed for isolated particles, can also be used as the basis for estimating the number of connected elements in a network by the Euler number (Gundersen et al. 1993), e.g., the number of lung alveoli (Ochs et al. 2004b, c; Knudsen et al. 2007, 2009) or the number of loops in the alveolar capillary network (Willführ et al. 2015).

EM in combination with stereology contributes significantly to our understanding of lung structure and function in health and disease, in particular when quantitative high-resolution structural data are correlated with other (e.g., physiological or biochemical) data to establish structure–function relationships in experimental studies when different groups (e.g., treated vs. untreated controls or transgenic vs. wild-type organisms) are compared. By this approach, surfactant dysfunction and the effects of exogenous surfactant therapy in animal models of lung transplantation-associated ischemia/reperfusion injury could be evaluated (Ochs et al. 1999, 2000; Mühlfeld et al. 2009, 2010).

A case study for the relevance of EM: collapse induration

The relevance of the combined EM/stereology approach in experimental studies may be illustrated in more detail by one recent example: the elucidation of the role of surfactant alterations and alveolar collapse for the early pathogenesis of lung fibrosis. The type II alveolar epithelial cell has been termed the "defender of the alveolus" (Mason and Williams 1977; Fehrenbach 2001) because of its two main functions: being the cellular source of surfactant and constituting the progenitor cell population of the alveolar epithelium. The progenitor function is particularly obvious in cases of acute lung injury/acute respiratory distress syndrome (Ware and Matthay 2000; Matthay and Zemans 2011). The histopathologic alterations are known as diffuse alveolar damage and involve an early exudative phase with alveolar epithelial injury, intraalveolar edema formation and surfactant alterations, and a late fibroproliferative phase with proliferation of type II alveolar epithelial cells (cuboidal metaplasia) and thickening of the alveolar septa (Bachofen and Weibel 1977; Ochs 2006b). The final outcome is either restoration or fibrosis. The current pathogenetic concept of lung fibrosis involves abnormal wound healing after repetitive alveolar epithelial injury (Gross and Hunninghake 2001; Selman et al. 2001). This concept is strongly supported by recent data showing that dysfunction of type II alveolar epithelial cells and thus of the surfactant system, e.g., mutations of genes encoding for surfactant protein C or the lipid transporter ABCA3 which is involved in the formation of lamellar bodies, leads to a fibrotic phenotype in patients (Günther et al. 2012; Uhal and Nguyen 2013; Mulugeta et al. 2015; Whitsett et al. 2015). The consequences of type II cell injury would be denudation of the alveolar epithelial basal lamina with subsequent cuboidal metaplasia of remaining type II cells as well as surfactant dysfunction with alveolar collapse due to increased surface tension. Alveolar collapse would then lead to a loss of "open" (i.e., ventilated) alveoli, a loss of aerated parenchymal lung volume, a loss of functional alveolar surface area available for gas exchange and a thickening of the alveolar septa. In fact, alveolar epithelial cell death and alveolar collapse in cases of human lung fibrosis have been shown previously by EM (Katzenstein 1985; Myers and Katzenstein 1988). Anna-Luise Katzenstein described "folding of portions of alveolar septa or collapse of entire alveoli and permanent apposition of their walls […] in areas that had been denuded of alveolar lining epithelium" and observed that type II alveolar epithelial cells "attempting to re-epithelialize the denuded basal lamina proliferated over the surface of apposed septa, thereby […] forming a single thickened septum" (Katzenstein 1985). However, historically this description was an independent rediscovery of the old pathogenetic concept of "collapse induration"—a term not used by Katzenstein (1985) or Myers and Katzenstein (1988). Collapse induration appeared in the English literature in a letter and two review articles by Arne Burkhardt (Burkhardt 1986, 1989; Burkhardt and Cottier 1989). He pointed out that "The central importance of alveolar collapse and its sequelae—permanent apposition of the denuded alveolar walls 'glued' together […], so-called *collapse induration* or *atelectatic induration*—for the pathogenesis of lung fibrosis has been vastly neglected in the international literature" (Burkhardt 1989) and that it had been known in the German literature for a long time. Indeed, in 1881 (the same year that Albert Kölliker published his seminal paper), Ernst Ziegler published a Pathology textbook ("Lehrbuch der allgemeinen und speciellen pathologischen Anatomie für Ärzte und Studirende") in which he entitled a paragraph "Atelectase, Collapsinduration und Emphysem" which contained a figure showing collapse induration (Ziegler 1881). This textbook was translated and published in English as "A textbook of pathological anatomy and pathogenesis" in 1884. Here, however, the term "Collapsinduration" was translated as "collapse" or "cirrhosis of collapse." Thus, it seems that the term was lost in translation until Burkhardt changed this more than 100 years later.

In order to obtain a better understanding of the role of surfactant dysfunction, alveolar collapse and collapse induration in the development of lung fibrosis, we performed an experimental study using the rat bleomycin model (Lutz et al. 2015). Although this animal model of lung fibrosis (like any other animal model of human disease) has clear limitations (Williamson et al. 2015), it allows to analyze the time course of quantitative structural alterations in relation to lung function during the progression from initial lung injury to fibrosis in a defined and reproducible manner. After injury induction with bleomycin, rats were analyzed in the early (1 and 3 days after injury) and the late (7 and 14 days after injury) phase. In the early phase, microatelectases with collapse of alveoli and their walls piling up were found. Lung elastance (a measure of stiffness) increased, but could be decreased when positive end-expiratory pressure (PEEP) was increased, suggesting that the collapsed alveoli were still recruitable. Type II alveolar epithelial cells were hypertrophic with increased volumes of intracellular surfactant. On the other hand, intraalveolar surfactant was decreased and biophysically less active. In the late phase, fibrosis with thickening of alveolar septa and collapse induration became obvious. Lung elastance further increased, but now could not be decreased by increasing PEEP, thus suggesting that collapsed alveoli were no longer recruitable and that the remaining ventilated lung parenchyma was overdistended. Comparison of stereological data from the early and late phase of injury showed an increase in non-ventilated parenchyma due to fibrotic tissue, a decrease in

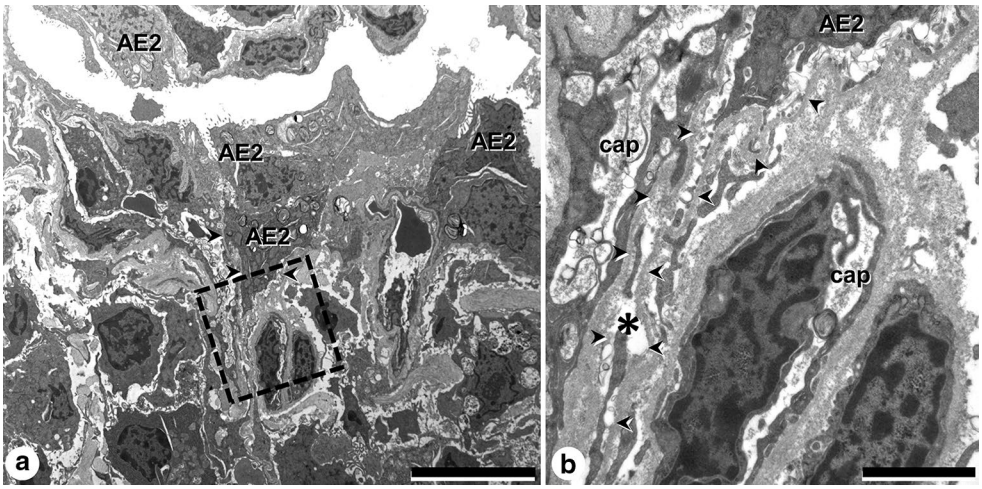

Fig. 1 Transmission electron microscopy. Human lung. Sample from an explanted lung of a patient with idiopathic pulmonary fibrosis undergoing lung transplantation (for details, see Lutz et al. 2015). **a** Collapse induration. Region with collapsed alveolus and cuboidal metaplasia of type II alveolar epithelial cells (AE2). An infolding of the alveolar epithelial basal lamina is "sealed" by an AE2 cell (*arrowheads*). **b** At higher magnification of the region indicated by *dashed lines* in **a**, the denuded epithelial basal lamina of the collapsed alveolus can be traced in detail (*arrowheads*). The former alveolar lumen (*asterisk*) is overgrown by an AE2 cell. The alveolar capillaries (cap) underneath the infolded basal lamina are isolated from the remaining ventilated airspaces. *Scale bars* 10 µm (**a**), 2 µm (**b**)

total alveolar airspace volume, a decrease in the number of ventilated alveoli closely correlated with a decrease in static compliance, an increase in the mean size of the remaining alveoli, a decrease in alveolar surface area and an increase in alveolar septal wall thickness at late phase. Interestingly, the presence of collapse induration could also be confirmed in samples from two explants from patients with idiopathic pulmonary fibrosis (IPF, the most common and most fatal form of lung fibrosis) that underwent lung transplantation (Fig. 1). Taken together, these findings clearly suggest that alveolar collapse and collapse induration are important events in the development of lung fibrosis. An initial alveolar epithelial injury with surfactant alterations leads to alveolar collapse which is at first reversible but then becomes irreversible and finally permanent due to collapse induration (Lutz et al. 2015).

In this case study, EM and stereology were essential for gaining mechanistic insight into the pathogenesis of fibrosis. The earlier findings by Katzenstein (1985) and the notions by Burkhardt (1986, 1989) show that this pathogenetic concept is not entirely new. Lung function tests in patients with fibrosing alveolitis indicated a loss of functioning alveoli ("lung shrinkage," Gibson and Pride 1977). Alveolar collapse into alveolar ducts has also been suggested as a relevant mechanism for the development of fibrosis, for example, by Crouch (1990), Hogg (1991), Galvin et al. (2010) and Leslie (2011). Moreover, permanent alveolar collapse into alveolar ducts would also explain the phenomenon of "honeycombing" (Galvin et al. 2010, Leslie 2011). Radiologically, it is defined as thick-walled cystic spaces of comparable diameters of typically 3–10 mm (Hansell et al. 2008). Honeycombing with a predominantly peripheral and basal distribution is a hallmark of the diagnosis of IPF based on computed tomography (CT). Indeed, the posterior basal segments of the lung should be the most severely involved, because these alveoli are the smallest in the upright and supine positions and are therefore more likely to collapse (Galvin et al. 2010). In addition, Coxson et al. (1997), using a combined CT and histopathology approach, reported a reduction in airspace volume and surface area without increase in lung tissue volume in IPF patients. Accordingly, no increase in total lung collagen could be found in IPF patients (Fulmer et al. 1980). Collectively, these data indicate that clinically manifest lung fibrosis is not primarily a disease of excess extracellular matrix production and deposition, but rather the final stage of a sequence of alveolar epithelial injury combined with surfactant dysfunction, alveolar collapse, collapse induration and scarring. This concept, which only seems new to those who do not look through the "retrospectroscope," has been elegantly reviewed recently by Todd et al. (2015). It should result in the identification of new therapeutic targets and the development of new treatment strategies for this devastating disease.

A look into the near future

From flatland to 3D EM: opportunities and challenges

A new dimension to lung EM was (literally) added by 3D techniques. The spectrum currently ranges from array

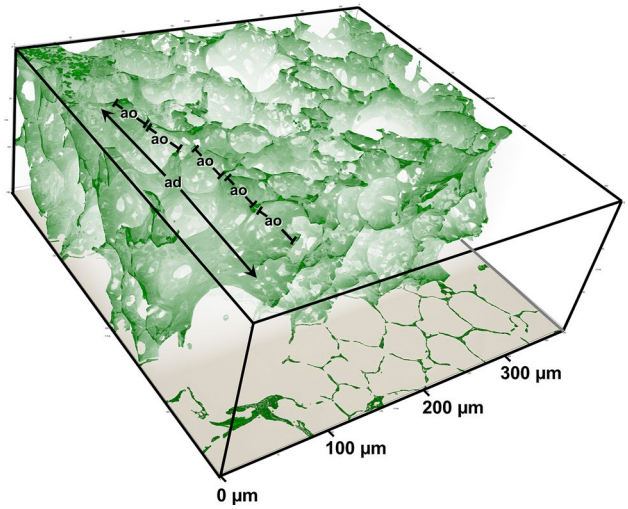

Fig. 2 Serial block face scanning electron microscopy. Mouse lung. Segmentation of alveolar septal walls from a stack of 2083 images (section thickness 70 nm) projected onto a single slice of the stack. Block size about 350 × 350 × 150 µm. The complexity of the branching acinar airways with alveolar ducts (ad) whose "wall" is entirely constituted by the 3D network of alveolar openings (ao) can be appreciated. Compare videos A1 and A2 in online supplement

tomography via serial block face scanning EM (SBF-SEM) and focused ion beam scanning EM (FIB-SEM) to electron tomography. These methods complement each other perfectly because they cover sample sizes from large to small and axial resolution from low to high. Strictly speaking, the first three methods are stacking methods, whereas only electron tomography is tomography in the strict sense (reconstruction from projection images). The first three methods are also, together with their pre-digital ancestor, serial section transmission EM, collectively referred to as volume EM (Briggman and Bock 2011; Peddie and Collinson 2014). In array tomography, ribbons of serial ultrathin sections are cut and collected on a solid substrate for imaging (e.g., by SEM). These images are then aligned and reconstructed in 3D (Micheva and Smith 2007; Wacker and Schroeder 2013). The most recent improvement in array tomography is an automated tape-collecting ultramicrotome (ATUM, Hayworth et al. 2014). SBF-SEM and FIB-SEM are both based on the principle of alternating scanning of the sample block surface and the removal of thin slices from that surface in the vacuum chamber. Therefore, they are both destructive because the slices are

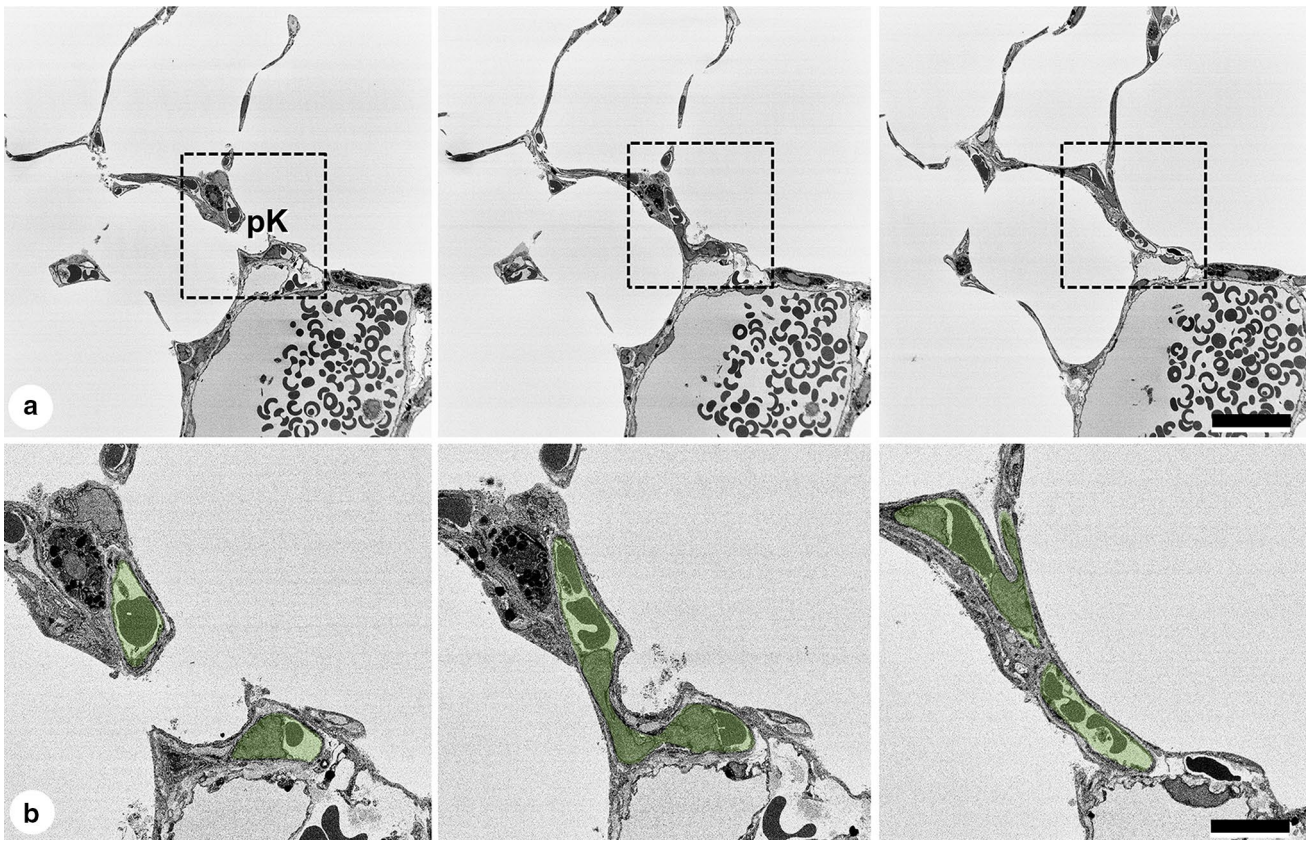

Fig. 3 Serial block face scanning electron microscopy. Mouse lung. Three single slices (numbers 343, 372 and 466) out of a stack of 1219 images (section thickness 50 nm) are shown. **a** Overview. The region with an interalveolar pore of Kohn (pK) indicated by the *dashed lines* is shown at higher magnification in **b**. Two segments of the alveolar capillary network (*highlighted in green*, *left*) connect (*middle*) and branch (*right*). Compare videos A3 and A4 in online supplement. *Scale bars* 30 µm (**a**), 10 µm (**b**)

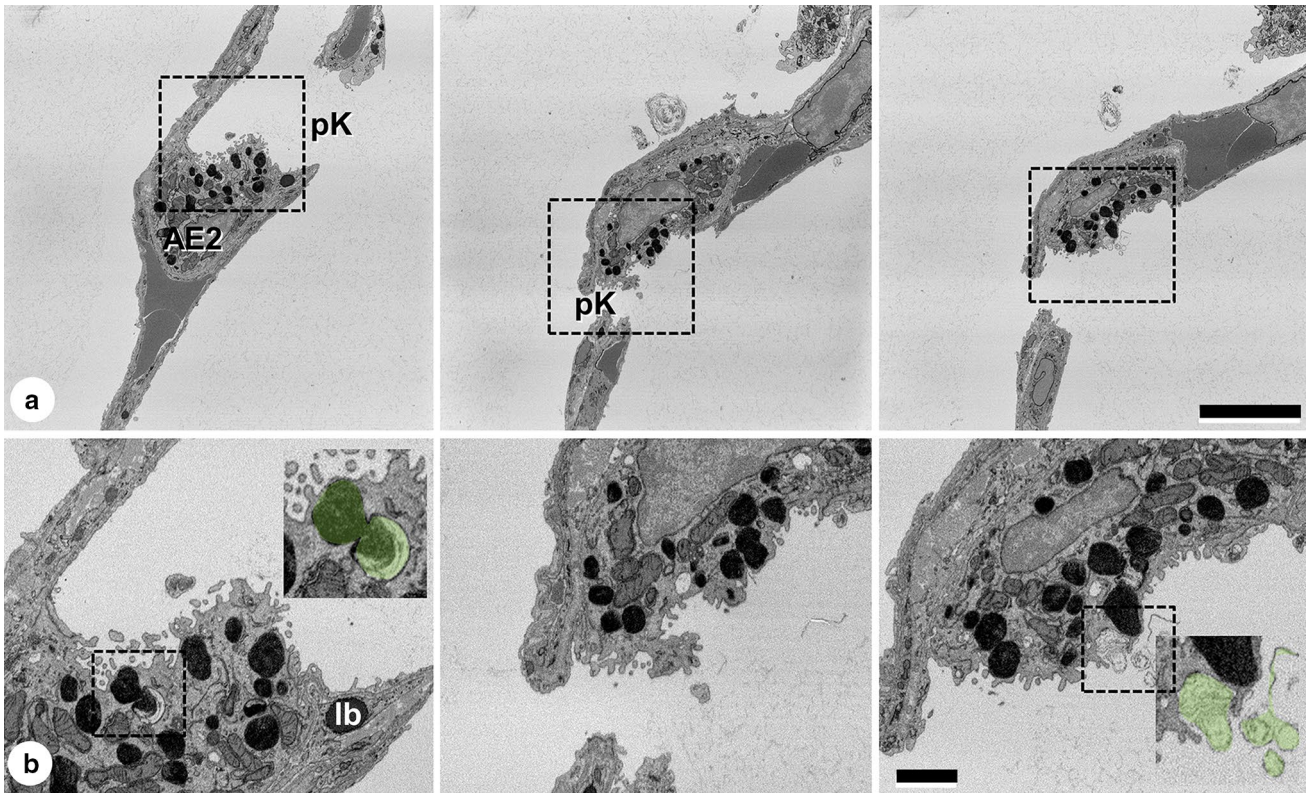

Fig. 4 Serial block face scanning electron microscopy. Mouse lung. Three single slices (numbers 26, 103 and 125) out of a stack of 224 images (section thickness 50 nm) are shown. **a** Overview. The region with the type II alveolar epithelial cell (AE2) indicated by the *dashed lines* is shown at higher magnification in **b**. The AE2 cell sits at the junction of three alveolar septa and two interalveolar pores of Kohn (pK). Its apical membrane is exposed toward the upper (*left*) as well as the lower (*middle* and *right*) alveolus. Intracellular surfactant material is stored in lamellar bodies (lb). Occasionally, fusions of lb prior to secretion (*left inset*, *highlighted in green*) and secretion of surfactant into the alveolar lumen (*right inset, highlighted in green*) can be observed. Compare videos A5 and A6 in online supplement. *Scale bars* 10 µm (**a**), 2 µm (**b**)

lost after removal, and thus, the recorded part of the sample is completely destroyed. In SBF-SEM, the removal is achieved by sectioning with an integrated ultramicrotome, and in FIB-SEM by milling with a focused gallium ion beam (Briggman and Bock 2011; Peddie and Collinson 2014). In electron tomography, a rotational relationship between detector (camera) and sample is created by tilting the section (typical thickness around 200–500 nm) inside the electron microscope at defined intervals producing a tilt series: a sequence of projections of the object from different angles. This tilt series is further processed to result in an electron tomogram, a stack of parallel slices with an axial resolution in the range of 2–5 nm. Particular structures of interest can then be segmented for further analysis (Bonetta 2005; McIntosh et al. 2005). It should also be noted that cryo-FIB-SEM can be used as a tool for preparing samples for cryo-electron tomography (Villa et al. 2013; Lucic et al. 2013).

These techniques provide 3D datasets much more efficiently than serial section transmission EM because the acquisition of raw datasets is done to a large extent automatically. After adaptation of fixation, processing and embedding protocols which may be required in particular for SBF-SEM and FIB-SEM in order to improve contrast and conductivity (Deerinck et al. 2010; Tapia et al. 2012), they are ready to be applied in order to gain new insights into the functional structure of the lung. With respect to the alveolar region of the lung, SBF-SEM allows visualization of alveolar sacs in 3D (Fig. 2 and Videos A1 and A2 in online supplement). The complex alveolar capillary network can also be traced (Fig. 3 and Videos A3 and A4 in online supplement). Type II alveolar epithelial cells can be followed in the z-direction, demonstrating the simultaneous secretion of surfactant material into two neighboring alveoli (Fig. 4 and Videos A5 and A6 in online supplement). The secretion of surfactant by single lamellar bodies can be studied by FIB-SEM (Fig. 5 and Video A7 in online supplement). Eventually, the arrangement of individual lamellae within lamellar bodies is discernible by electron tomography (Fig. 6 and Video A8 in online supplement).

Relevant subjects for future applications may include high-resolution reconstructions of complete type I alveolar

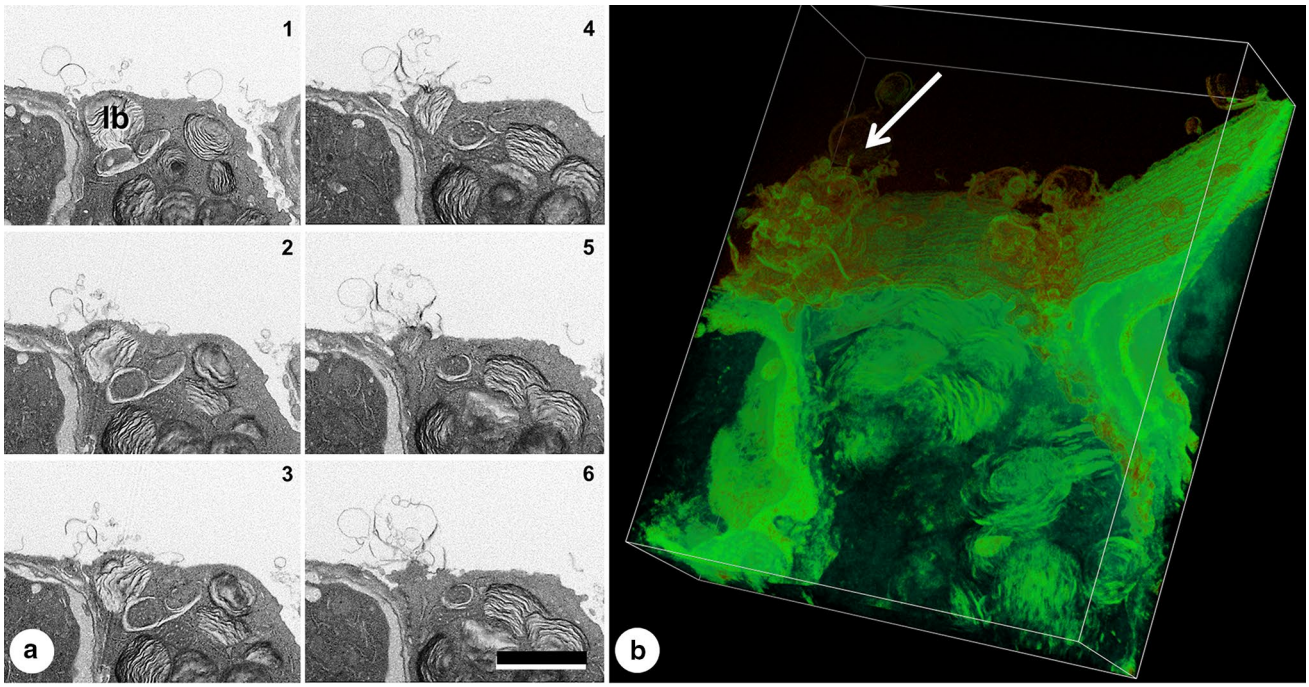

Fig. 5 Focused ion beam scanning electron microscopy. Mouse lung. Six single slices (numbers 62, 86, 91, 113, 129 and 133) out of a stack of 191 images (milling thickness 10 nm) showing the apical part of a type II alveolar epithelial cell are shown (**a**). The fusion of a lamellar body (lb) with the apical membrane and the secretion of surfactant into the alveolar lumen can be followed in *z*-direction. **b** Segmentation of the *z* stack showing secreted surfactant material (*arrow*). Compare video A7 in online supplement. *Scale bar* 1 µm

epithelial cells in order to visualize the complexity of their thin cell sheets—the reason why Albert Kölliker believed that "non-nucleated plates" exist in the alveolar epithelium. It would also be of considerable interest to understand the development of type I cells and the transformation of type II into type I cells during regeneration after lung injury. Another potential application relates to the complex alveolar capillary network, its development and postnatal remodeling during the phase of microvascular maturation. Finally, in cases of lung fibrosis it is still unclear how connected regions of collapse induration and scarring with fibroblastic foci are. Based on imaging methods with considerably lower resolution, there are opposing views whether fibroblastic foci form a reticulum (Cool et al. 2006) or not (Jones et al. 2016).

There is great potential in combining these 3D EM techniques with stereology because they have "built-in" datasets (3D stacks of thin slices) for stereological methods that require depth information like the Cavalieri estimator for volume estimation or the "optical" disector for number estimation. The combination of 3D EM and stereology to quantitative 3D EM is a true symbiosis (Vanhecke et al. 2007) as demonstrated by several studies with SBF-SEM (e.g., Shomorony et al. 2015), FIB-SEM (e.g., Merchan-Perez et al. 2009) and electron tomography (e.g., Vanhecke et al. 2007). This approach is part of the concept of "morphomics" (Lucocq et al. 2015; Mayhew and Lucocq 2015).

Current analysis strategies in EM are either "top-down" (zooming in by correlative microscopy from whole organisms via organs and tissues down to the cellular and subcellular level) or "bottom-up" (structural biology of molecules by single-particle cryo-EM, Eisenstein 2016). There is still a gap between these two approaches which are not (yet) fully connected. The fitting of molecular data into a whole cellular and supracellular context by cryo-electron tomography, although under current development as "visual proteomics" (Baumeister 2002; Nickell et al. 2006; Lucic et al. 2008, 2013), awaits to be established for the lung.

A word of caution is necessary regarding the amount of digital data that can be produced by 3D EM techniques. "Big data" may not necessarily mean "big information," and before producing huge amounts of digital waste, one should evaluate the amount of data which is sufficient in order to get the information that is actually relevant in the context of a given study. Here, again, stereology may prove to be useful because it provides smart sampling strategies (see Lucocq et al. 2015).

In order to understand the lung, we have to look into it (Weibel 1979b), and the closer we look, the more we may be able to see (Ochs 2010). Biomedical EM is an ever-developing and vital field (Knott and Genoud 2013). The

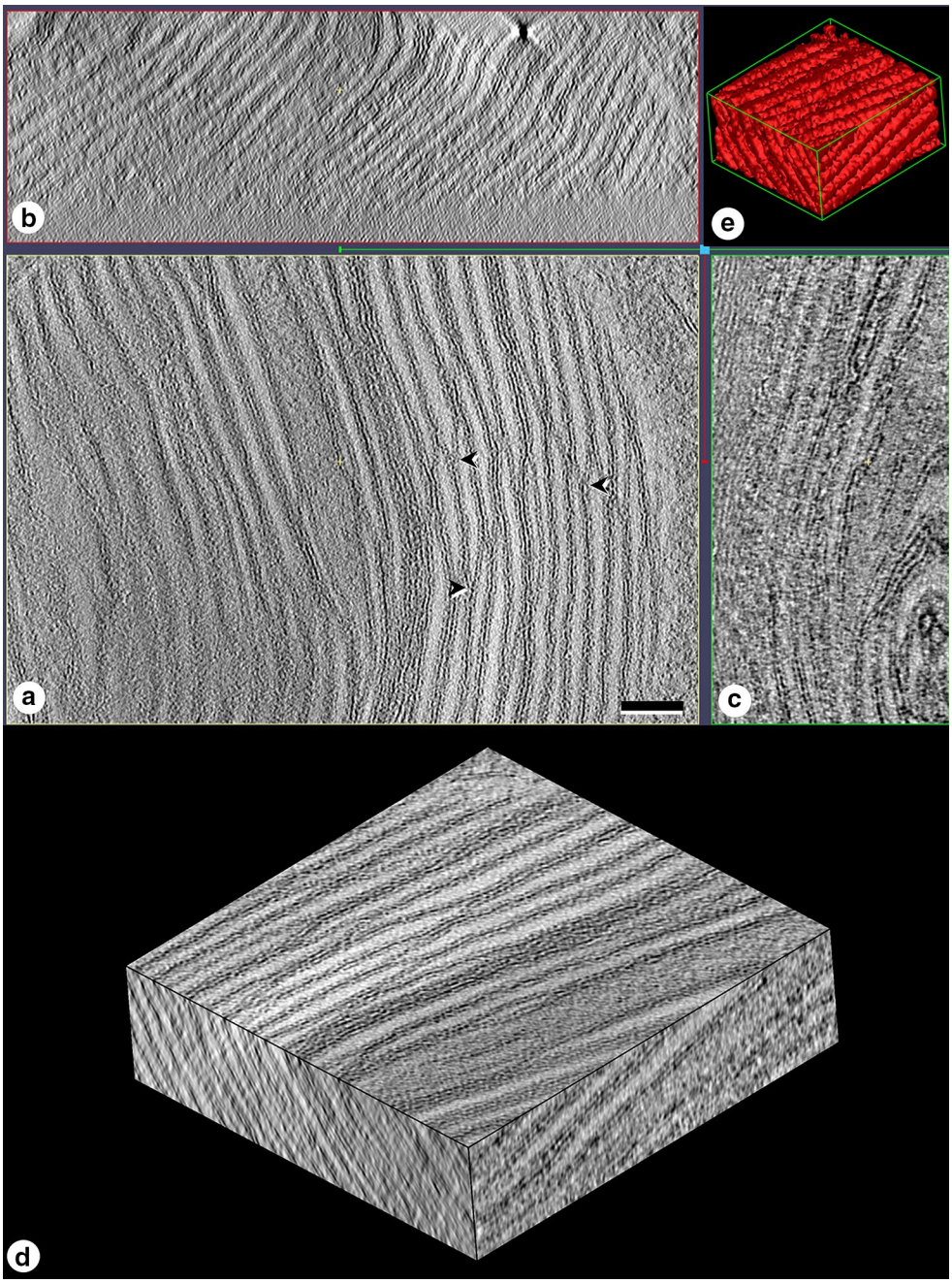

Fig. 6 Electron tomography. Mouse lung. A single slice of the tomogram (reconstructed from a tilt series of 101 images recorded with an increment of 1° from a section of 300-nm thickness) shows individual lamellae representing surfactant material inside a lamellar body (**a**). Occasionally, lamellar bifurcations are visible (*arrowheads*). Besides slices in *xy* direction (**a**), lateral views can also be generated in *xz* (**b**), in *yz* (**c**) or in any preferred direction at any preferred position in the 3D data stack. Individual volumes can be reconstructed (**d**) and segmented (**e**). Compare video A8 in online supplement. *Scale bar* 100 nm

high resolution provided by EM remains unparalleled (Pavelka and Roth 2015). Moreover, EM has the unique advantage of providing an "open view" into cells and tissues within their full architectural context, now even in 3D, which leaves room for surprising findings leading into new and unexpected directions—an important aspect in many cases of important scientific discoveries (Comroe 1977). This is in contrast to techniques where only those structures are visualized which were a priori targeted by—hopefully specific (Griffiths and Lucocq 2014)—fluorescent labels. New technological developments and improvements will shed new light (actually, electrons) on molecules, cells,

tissues and organs. We can therefore expect that EM will remain an indispensable tool for a better understanding of the functional design of the lung.

Acknowledgments Work from the authors' laboratory was and is funded by the German Research Federation (DFG: OC23/7-3, 8-1, 9-3, 10-1; MU3118/2-1, KN916/1-1, SFB 587/TP B18; INST 192/504-1, INST 193/57-1; REBIRTH Cluster of Excellence), the Federal Ministry for Education and Research (BMBF: German Center for Lung Research DZL; 01DG14009) and the Swiss National Science Foundation (SNF: 116417, 121390, CRSII3_160704/1). The authors thank Dr. Hubert Schulz at the Training, Application and Support Center (TASC) of Carl Zeiss Microscopy, Oberkochen, Germany, for expert technical help with the FIB image acquisition and the generation of raw data sets at the Zeiss Application Center.

Compliance with ethical standards

Conflict of interest The authors declare that they have no conflict of interest.

References

Al-Amoudi A, Chang JJ, Leforestier A, McDowall A, Salamin LM, Norlen LPO, Richter K, Blanc NS, Studer D, Dubochet J (2004) Cryo-electron microscopy of vitreous sections. EMBO J 23:3583–3588

Allen TD (2008) Introduction to electron microscopy for biologists. Methods in cell biology, vol 88. Elsevier, Amsterdam

Bachofen M, Weibel ER (1977) Alterations of the gas exchange apparatus in adult respiratory insufficiency associated with sepitcemia. Am Rev Respir Dis 116:589–615

Baddeley A, Vedel Jensen EB (2005) Stereology for statisticians. Chapman & Hall, Boca Raton

Bauer R (1988) Electron spectroscopic imaging: an advanced technique for imaging and analysis in transmission electron microscopy. Meth Microbiol 20:113–146

Baumeister W (2002) Electron tomography: towards visualizing the molecular organization of the cytoplasm. Curr Opin Struct Biol 12:679–684

Bendayan M (2001) Worth its weight in gold. Science 291:1363–1365

Bendayan M, Roth J, Perrelet A, Orci L (1980) Quantitative immunocytochemical localization of pancreatic secretory proteins in subcellular compartments of the rat acinar cell. J Histochem Cytochem 28:149–160

Bonetta L (2005) Zooming in on electron tomography. Nat Methods 2:139–144

Brandenberger C, Ochs M, Mühlfeld C (2015) Assessing particle and fiber toxicology in the respiratory system: the stereology toolbox. Part Fibre Toxicol 12(35):1–15

Brasch F, ten Brinke A, Johnen G, Ochs M, Kapp N, Müller KM, Beers MF, Fehrenbach H, Richter J, Batenburg JJ, Bühling F (2002) Involvement of cathepsin H in the processing of the hydrophobic surfactant-associated protein C in type II pneumocytes. Am J Respir Cell Mol Biol 26:659–670

Brasch F, Ochs M, Kähne T, Guttentag S, Schauer-Vukasinovic V, Derrick M, Johnen G, Kapp N, Müller KM, Richter J, Giller T, Hawgood S, Bühling F (2003) Involvement of napsin A in the C- and N-terminal processing of surfactant protein B in type-II-pneumocytes of the human lung. J Biol Chem 278:49006–49014

Brasch F, Johnen G, Winn-Brasch A, Guttentag SH, Schmiedl A, Kapp N, Suzuki Y, Müller KM, Richter J, Hawgood S, Ochs M (2004) Surfactant protein B in type II pneumocytes and intra-alveolar surfactant forms of human lungs. Am J Respir Cell Mol Biol 30:449–458

Briggman KL, Bock DD (2011) Volume electron microscopy for neuronal circuit reconstruction. Curr Opin Neurobiol 22:154–161

Burkhardt A (1986) Pathogenesis of pulmonary fibrosis. Hum Pathol 17:971–973

Burkhardt A (1989) Alveolitis and collapse in the pathogenesis of pulmonary fibrosis. Am Rev Respir Dis 140:513–524

Burkhardt A, Cottier H (1989) Cellular events in alveolitis and the evolution of pulmonary fibrosis. Virchows Arch B Cell Pathol 58:1–13

Carlson EC (1999) Frank N. Low: gentle giant of electron microscopy (1911–1998). Anat Rec 257:48–49

Cavalier A, Spehner D, Humbel BM (2009) Handbook of cryo-preparation methods for electron microscopy. CRC Press, Boca Raton

Clements JA (1957) Surface tension of lung extracts. Proc Soc Exp Biol Med 95:170–172

Clements JA (1997) Lung surfactant: a personal perspective. Annu Rev Physiol 59:1–21

Comroe JH (1977) Retrospectroscope. Insights into medical discovery. Von Gehr Press, Menlo Park

Cool CD, Groshong SD, Rai PR, Henson PM, Stewart JS, Brown KK (2006) Fibroblast foci are not discrete sites of lung injury or repair. The fibroblast reticulum. Am J Respir Crit Care Med 174:654–658

Coxson HO, Hogg JC, Mayo JR, Behzad H, Whittall KP, Schwartz DA, Hartley PG, Galvin JR, Wilson JS, Hunninghake GW (1997) Quantification of idiopathic pulmonary fibrosis using computed tomography and histology. Am J Respir Crit Care Med 155:1649–1656

Crouch E (1990) Pathobiology of pulmonary fibrosis. Am J Physiol Lung Cell Mol Physiol 259:L159–L184

Cruz-Orive LM (1987) Stereology: historical notes and recent evolution. Acta Stereol 6:43–56

Deerinck T, Bushong E, Lev-Ram V, Shu X, Tsien R, Ellisman M (2010) Enhancing serial block-face scanning electron microscopy to enable high resolution 3-D nanohistology of cells and tissues. Microsc Microanal 16:1138–1139

Dubochet J (2012) Cryo-EM—the first 30 years. J Microsc 245:221–224

Eisenstein M (2016) The field that came from the cold. Nat Methods 13:19–22

Fehrenbach H (2001) Alveolar epithelial type II cell: defender of the alveolus revisited. Respir Res 2:33–46

Fehrenbach H, Ochs M, Richter J (1995) Energy-filtering TEM in the fine-structural study of the mammalian lung. Microsc Anal 37:11–14

Fulmer JD, Bienkowski RS, Cowan MJ, Breul SD, Bradley KM, Ferrans VJ, Roberts WC, Crystal RG (1980) Collagen concentration and rates of synthesis in idiopathic pulmonary fibrosis. Am Rev Respir Dis 122:289–301

Galvin JR, Frazier AA, Franks TJ (2010) Collaborative radiologic and histopathologic assessment of fibrotic lung disease. Radiology 255:692–706

Gibson GJ, Pride NB (1977) Pulmonary mechanics in fibrosing alveolitis. The effects of lung shrinkage. Am Rev Respir Dis 116:637–647

Gil J, Weibel ER (1969/1970) Improvements in demonstration of lining layer of lung alveoli by electron microscopy. Respir Physiol 8:13–36

Griffiths G (1993) Fine structure immunocytochemistry. Springer, Berlin

Griffiths G, Lucocq JM (2014) Antibodies for immunolabeling by light and electron microscopy: not for the faint hearted. Histochem Cell Biol 142:347–360

Gross TJ, Hunninghake GW (2001) Idiopathic pulmonary fibrosis. N Engl J Med 345:517–525

Gundersen HJG, Boyce RW, Nyengaard JR, Odgaard A (1993) The conneulor: unbiased estimation of connectivity using physical disectors under projection. Bone 14:217–222

Günther A, Korfei M, Mahavadi P, von der Beck D, Ruppert C, Markart P (2012) Unraveling the progressive pathophysiology of idiopathic pulmonary fibrosis. Eur Respir Rev 21:152–160

Hansell DM, Bankier AA, MacMahon H, McLoud TC, Müller NL, Remy J (2008) Fleischner society: glossary of terms for thoracic imaging. Radiology 246:697–722

Hayworth KJ, Morgan JL, Schalek R, Berger DR, Hildebrand DGC, Lichtman JW (2014) Imaging ATUM ultrathin section libraries with WaferMapper: a multi-scale approach to EM reconstruction of neural circuits. Front Neural Circuits 8(68):1–18

Hogg JC (1991) Chronic interstitial lung disease of unknown cause: a new classification based on pathogenesis. Am J Roentgenol 156:225–233

Howard CV, Reed MG (2005) Unbiased stereology. Three-dimensional measurement in microscopy, 2nd edn. Bios, Oxford

Hsia CCW, Hyde DM, Ochs M, Weibel ER (2010) An official research policy statement of the American Thoracic Society/European Respiratory Society: standards for quantitative assessment of lung structure. Am J Respir Crit Care Med 181:394–418

Hsia CCW, Hyde DM, Weibel ER (2016) Lung structure and the intrinsic challenges of gas exchange. Comp Physiol 6:827–895

Jones MG, Fabre A, Schneider P, Cinetto F, Sgalla G, Mavrogordato M, Jogai S, Alzetani A, Marshall BG, O'Reilly KMA, Warner JA, Lackie PM, Davies DE, Hansell DM, Nicholson AG, Sinclair I, Brown KK, Richeldi L (2016) Three-dimensional characterization of fibroblastic foci in idiopathic pulmonary fibrosis. JCI Insight 1(5):pii: e86375

Jung A, Allen L, Nyengaard JR, Gundersen HJG, Richter J, Hawgood S, Ochs M (2005) Design-based stereological analysis of the lung parenchymal architecture and alveolar type II cells in surfactant protein A and D double deficient mice. Anat Rec 286:885–890

Katzenstein AL (1985) Pathogenesis of "fibrosis" in interstitial pneumonia: an electron microscopic study. Hum Pathol 16:1015–1024

Knott G, Genoud C (2013) Is EM dead? J Cell Sci 126:4545–4552

Knudsen L, Ochs M, Mackay RM, Townsend P, Deb R, Mühlfeld C, Richter J, Gilbert F, Hawgood S, Reid K, Clark H (2007) Truncated recombinant human SP-D attenuates emphysema and type II cell changes in SP-D deficient mice. Respir Res 8(70):1–12

Knudsen L, Wucherpfennig K, Mackay RM, Townsend P, Mühlfeld C, Richter J, Hawgood S, Reid K, Clark H, Ochs M (2009) A recombinant fragment of human surfactant protein D lacking the short collagen-like stalk fails to correct morphological alterations in lungs of SP-D deficient mice. Anat Rec 292:183–189

Kölliker A (1881) Zur Kenntniss des Baues der Lunge des Menschen. Verh d Phys Med Ges Würzburg N.F.16:1–24

Koster AJ, Klumperman J (2003) Electron microscopy in cell biology: integrating structure and function. Nat Rev Mol Cell Biol 4(Suppl.):SS6–SS10

Kuo J (2014) Electron microscopy. Methods and protocols, 3rd edn. Humana Press, New York

Leapman RD, Ornberg RL (1988) Quantitative electron energy loss spectroscopy in biology. Ultramicroscopy 24:251–268

Leslie KO (2011) Idiopathic pulmonary fibrosis may be a disease of recurrent, tractional injury to the periphery of the aging lung. Arch Pathol Lab Med 135:1–10

Liou W, Geuze HJ, Slot JW (1996) Improving structural integrity of cryosections for immunogold labeling. Histochem Cell Biol 106:41–58

Low FN (1952) Electron microscopy of the rat lung. Anat Rec 113:437–444

Low FN (1953) The pulmonary alveolar epithelium of laboratory animals and man. Anat Rec 117:241–264

Lucic V, Leis A, Baumeister W (2008) Cryo-electron tomography of cells: connecting structure and function. Histochem Cell Biol 130:185–196

Lucic V, Rigort A, Baumeister W (2013) Cryo-electron tomography: the challenge of doing structural biology in situ. J Cell Biol 202:407–419

Lucocq JM, Mayhew TM, Schwab Y, Steyer AM, Hacker C (2015) Systems biology in 3D space—enter the morphome. Trends Cell Biol 25:59–64

Lutz D, Gazdhar A, Lopez-Rodriguez E, Ruppert C, Mahavadi P, Günther A, Klepetko W, Bates JH, Smith B, Geiser T, Ochs M, Knudsen L (2015) Alveolar derecruitment and collapse induration as crucial mechanisms in lung injury and fibrosis. Am J Respir Cell Mol Biol 52:232–243

Mason RJ, Williams MC (1977) Type II alveolar cell: defender of the alveolus. Am Rev Respir Dis 115:81–91

Matthay MA, Zemans RL (2011) The acute respiratory distress syndrome: pathogenesis and treatment. Annu Rev Pathol Mech Dis 6:147–163

Mayhew TM (2015) Quantitative immunocytochemistry at the ultrastructural level: a stereology-based approach to molecular nanomorphomics. Cell Tissue Res 360:43–59

Mayhew TM, Lucocq JM (2008) Developments in cell biology for quantitative immunoelectron microscopy based on thin sections: a review. Histochem Cell Biol 130:299–313

Mayhew TM, Lucocq JM (2015) From gross anatomy to the nanomorphome: stereological tools provide a paradigm for advancing research in quantitative morphomics. J Anat 226:309–321

Mayhew TM, Mühlfeld C, Vanhecke D, Ochs M (2009) A review of recent methods for efficiently quantifying immunogold and other nanoparticles using TEM sections through cells, tissues and organs. Ann Anat 191:153–170

McIntosh JR (2007) Cellular electron microscopy. Methods in cell biology, vol 79. Elsevier, Amsterdam

McIntosh R, Nicastro D, Matronarde D (2005) New views of cells in 3D: an introduction to electron tomography. Trends Cell Biol 15:43–51

Merchan-Perez A, Rodriguez JR, Alonso-Nanclares L, Schertel A, DeFilipe J (2009) Counting synapses using FIB/SEM microscopy: a true revolution for ultrastructural volume reconstruction. Front Neuroanat 2(18):1–14

Micheva KD, Smith SJ (2007) Array tomography: a new tool for imaging the molecular architecture and ultrastructure of neural circuits. Neuron 55:25–36

Miller WS (1937) The lung. Charles C Thomas, Springfield

Möbius W (2009) Cryopreparation of biological specimens for immunoelectron microscopy. Ann Anat 191:231–247

Moor H, Bellin G, Sandri C, Akert K (1980) The influence of high pressure freezing on mammalian nerve tissue. Cell Tissue Res 209:201–216

Mühlfeld C, Ochs M (2013) Quantitative microscopy of the lung: a problem-based approach. Part 2: stereological parameters and study designs in various diseases of the respiratory tract. Am J Physiol Lung Cell Mol Physiol 305:L205–L221

Mühlfeld C, Rothen-Rutishauser B, Vanhecke D, Blank F, Gehr P, Ochs M (2007) Visualization and quantitative analysis of nanoparticles in the respiratory system by transmission electron microscopy. Part Fibre Toxicol 4(11):1–17

Mühlfeld C, Schaefer IM, Becker L, Bussinger C, Vollroth M, Bosch A, Nagib R, Madershahian N, Richter J, Wahlers T, Wittwer T, Ochs M (2009) Pre-ischaemic exogenous surfactant reduces pulmonary injury in rat ischaemia/reperfusion. Eur Respir J 33:625–633

Mühlfeld C, Becker L, Bussinger C, Vollroth M, Nagib R, Schaefer IM, Knudsen L, Richter J, Madershahian N, Wahlers T, Wittwer T, Ochs M (2010) Exogenous surfactant in ischemia/reperfusion: effects on endogenous surfactant pools. J Heart Lung Transplant 29:327–334

Mühlfeld C, Hegermann J, Wrede C, Ochs M (2015) A review of recent developments and applications of morphometry/stereology in lung research. Am J Physiol Lung Cell Mol Physiol 309:L526–L536

Mulugeta S, Nureki SI, Beers MF (2015) Lost after translation: insights from pulmonary surfactant for understanding the role of alveolar epithelial dysfunction and cellular quality control in fibrotic lung disease. Am J Physiol Lung Cell Mol Physiol 309:L507–L525

Myers JL, Katzenstein AL (1988) Epithelial necrosis and alveolar collapse in the pathogenesis of usual interstitial pneumonia. Chest 94:1309–1311

Nickell S, Kofler C, Leis AP, Baumeister W (2006) A visual approach to proteomics. Nat Rev Mol Cell Biol 7:225–230

Ochs M (2006a) A brief update on lung stereology. J Microsc 222:188–200

Ochs M (2006b) Stereological analysis of acute lung injury. Eur Respir Rev 15:115–121

Ochs M (2010) The closer we look the more we see? Quantitative microscopic analysis of the pulmonary surfactant system. Cell Physiol Biochem 25:27–40

Ochs M, Mühlfeld C (2013) Quantitative microscopy of the lung: a problem-based approach. Part 1: basic principles of lung stereology. Am J Physiol Lung Cell Mol Physiol 305:L15–L22

Ochs M, Weibel ER (2015) Functional design of the human lung for gas exchange. In: Grippi MA, Elias JA, Fishman JA, Kotloff RM, Pack AI, Senior RM (eds) Fishman's pulmonary diseases and disorders, 5th edn. McGraw-Hill, New York, pp 20–62

Ochs M, Fehrenbach H, Richter J (1994) Electron spectroscopic imaging (ESI) and electron energy loss spectroscopy (EELS) of multilamellar bodies and multilamellar body-like structures in tannic acid-treated alveolar septal cells. J Histochem Cytochem 42:805–809

Ochs M, Nenadic I, Fehrenbach A, Albes JM, Wahlers T, Richter J, Fehrenbach H (1999) Ultrastructural alterations in intraalveolar surfactant subtypes after experimental ischemia and reperfusion. Am J Respir Crit Care Med 160:718–724

Ochs M, Fehrenbach H, Nenadic I, Bando T, Fehrenbach A, Schepelmann D, Albes JM, Wahlers T, Richter J (2000) Preservation of intraalveolar surfactant in a rat lung ischaemia/reperfusion injury model. Eur Respir J 15:526–531

Ochs M, Fehrenbach H, Richter J (2001) Ultrastructure of canine type II pneumocytes during hypothermic ischemia of the lung—a study by means of conventional and energy filtering transmission electron microscopy and stereology. Anat Rec 263:118–126

Ochs M, Johnen G, Müller KM, Wahlers T, Hawgood S, Richter J, Brasch F (2002) Intracellular and intraalveolar localization of surfactant protein A (SP-A) in the human lung. Am J Respir Cell Mol Biol 26:91–98

Ochs M, Fehrenbach H, Richter J (2004a) Occurence of lipid bodies in canine type II pneumocytes during hypothermic lung ischemia. Anat Rec 277:287–297

Ochs M, Knudsen L, Allen L, Stumbaugh A, Levitt S, Nyengaard JR, Hawgood S (2004b) GM-CSF mediates alveolar epithelial type II changes, but not emphysema-like pathology, in SP-D deficient mice. Am J Physiol Lung Cell Mol Physiol 287:L1333–L1341

Ochs M, Nyengaard JR, Jung A, Knudsen L, Voigt M, Wahlers T, Richter J, Gundersen HJG (2004c) The number of alveoli in the human lung. Am J Respir Crit Care Med 169:120–124

Pavelka M, Roth J (2015) Functional ultrastructure Atlas of tissue biology and pathology, 3rd edn. Springer, Vienna

Peddie CJ, Collinson LM (2014) Exploring the third dimension: volume electron microscopy comes of age. Micron 61:9–19

Reimer L (1991) Energy-filtering transmission electron microscopy. Adv Electron Electron Phys 81:43–126

Roth J (1989) Postembedding labeling on Lowicryl K4 M tissue sections: detection and modification of cellular components. In: Tartakoff AM (ed) Vesicular transport, methods in cell biology, vol 31. Academic Press, Oxford, pp 513–551

Roth J (1996) The silver anniversary of gold: 25 years of the collidal gold marker system for immunocytochemistry and histochemistry. Histochem Cell Biol 106:1–8

Roth J, Bendayan M, Orci L (1978) Ultrastructural localization of intracellular antigens by the use of protein A-gold complex. J Histochem Cytochem 26:1074–1081

Roth J, Bendayan M, Carlemalm E, Villiger W, Garavito M (1981) Enhancement of structural preservation and immunocytochemical staining in low temperature embedded pancreatic tissue. J Histochem Cytochem 29:663–671

Selman M, King TE, Pardo A (2001) Idiopathic pulmonary fibrosis: prevailing and evolving hypotheses about its pathogenesis and implications for therapy. Ann Intern Med 134:136–151

Shomorony A, Pfeifer CR, Aronova MA, Zhang G, Cai T, Xu H, Notkins AL, Leapman RD (2015) Combining quantitative 2D and 3D image analysis in the serial block face SEM: application to secretory organelles of pancreatic islet cells. J Microsc 259:155–164

Sterio DC (1984) The unbiased estimation of number and sizes or arbitrary particles using the disector. J Microsc 134:127–136

Studer D, Graber W, Al-Amoudi A, Eggli P (2001) A new approach for cryofixation by high-pressure freezing. J Microsc 203:285–294

Studer D, Humbel B, Chiquet M (2008) Electron microscopy of high pressure frozen samples: bridging the gap between cellular ultrastructure and atomic resolution. Histochem Cell Biol 130:877–889

Tapia JC, Kasthuri N, Hayworth KJ, Schalek R, Lichtman JW, Smith SJ, Buchanan JA (2012) High-contrast en bloc staining of neuronal tissue for field emission scanning electron microscopy. Nat Protocols 7:193–206

Todd NW, Atamas SP, Luzina IG, Galvin JR (2015) Permanent alveolar collapse is the predominant mechanism in idiopathic pulmonary fibrosis. Exp Rev Respir Med 9:411–418

Uhal BD, Nguyen H (2013) The Witschi hypothesis revisited after 35 years: genetic proof from SP-C BRICHOS domain mutations. Am J Physiol Lung Cell Mol Physiol 305:L906–L911

Vanhecke D, Studer D, Ochs M (2007) Stereology meets electron tomography: towards quantitative 3D electron microscopy. J Struct Biol 159:443–450

Vanhecke D, Herrmann G, Graber W, Hillmann-Marti T, Mühlfeld C, Studer D, Ochs M (2010) Lamellar body ultrastructure revisited: high-pressure freezing and cryo-electron microscopy of vitreous sections. Histochem Cell Biol 134:319–326

Villa E, Schaffer M, Plitzko JM, Baumeister W (2013) Opening windows into the cell: focused-ion-beam milling for cryo-electron tomography. Curr Opin Struct Biol 23:771–777

Voorhout WF, Weaver TE, Haagsman HP, Geuze HJ, Van Golde LM (1993) Biosynthetic routing of pulmonary surfactant proteins in alveolar type II cells. Microsc Res Tech 26:366–373

Wacker I, Schroeder RR (2013) Array tomography. J Microsc 252:93–99
Ware LB, Matthay MA (2000) The acute respiratory distress syndrome. N Engl J Med 342:1334–1349
Weibel ER (1963) Morphometry of the human lung. Academic Press, New York
Weibel ER (1971) The mystery of "non-nucleated plates" in the alveolar epithelium of the lung explained. Acta Anat 78:425–443
Weibel ER (1973) Morphological basis of alveolar-capillary gas exchange. Physiol Rev 53:419–495
Weibel ER (1979a) Stereological methods. Practical methods for biological morphometry, vol 1. Academic Press, London
Weibel ER (1979b) Fleischner lecture. Looking into the lung: what can it tell us? Am J Roentgenol 133:1021–1031
Weibel ER (1980) Stereological methods. Theoretical foundations, vol 2. Academic Press, London
Weibel ER (1984) The pathway for oxygen. Structure and function in the mammalian respiratory system. Harvard University Press, Cambridge
Weibel ER (1992) Stereology in perspective: a mature science evolves. Acta Stereol 11:1–13
Weibel ER (1996) The structural basis of lung function. In: West JB (ed) Respiratory physiology. People and ideas. Oxford University Press, New York, pp 3–46
Weibel ER (2013) A retrospective of lung morphometry: from 1963 to present. Am J Physiol Lung Cell Mol Physiol 305:L405–L408
Weibel ER (2015) On the tricks alveolar epithelial cells play to make a good lung. Am J Respir Crit Care Med 191:504–513
Weibel ER, Gil J (1968) Electron microscopic demonstration of an extracellular duplex lining layer of alveoli. Respir Physiol 4:42–57
Weibel ER, Gomez DM (1962) Architecture of the human lung. Use of quantitative methods establishes fundamental relations between size and number of lung structures. Science 137:577–585
Weibel ER, Palade GE (1964) New cytoplasmic components in arterial endothelia. J Cell Biol 23:101–112
Weibel ER, Kistler GS, Töndury G (1966) A stereologic electron microscope study of "tubular myelin figures" in alveolar fluids of rat lungs. Z Zellforsch Mikrosk Anat 69:418–427
Weibel ER, Hsia CCW, Ochs M (2007) How much is there really? Why stereology is essential in lung morphometry. J Appl Physiol 102:459–467
West JB (2016) Frank Low and the first images of the ultrastructure of the pulmonary blood-gas barrier. Am J Physiol Lung Cell Mol Physiol 310:L387–L392
Whitsett JA, Wert SE, Weaver TE (2015) Diseases of pulmonary surfactant homeostasis. Annu Rev Pathol Mech Dis 10:371–393
Willführ A, Brandenberger C, Piatkowski T, Grothausmann G, Nyengaard JR, Ochs M, Mühlfeld C (2015) Estimation of the number of alveolar capillaries by the Euler number (Euler-Poincaré characteristic). Am J Physiol Lung Cell Mol Physiol 309:L1286–L1293
Williamson JD, Sadofsky LR, Hart SP (2015) The pathogenesis of bleomycin-induced lung injury in animals and its applicability to human idiopathic pulmonary fibrosis. Exp Lung Res 41:57–73
Ziegler E (1881) Lehrbuch der allgemeinen und speciellen pathologischen Anatomie für Ärzte und Studirende. Gustav Fischer, Jena